Preferential Sampling of Elastic Chains in Turbulent Flows

Jason R. Picardo,[1,*] Dario Vincenzi,[2,†] Nairita Pal,[3,‡] and Samriddhi Sankar Ray[1,§]
[1]International Centre for Theoretical Sciences, Tata Institute of Fundamental Research, Bangalore 560089, India
[2]Université Côte d'Azur, CNRS, LJAD, Nice 06100, France
[3]Center for Nonlinear Studies, Los Alamos National Laboratory, Los Alamos, New Mexico 87545, USA

(Received 29 July 2018; published 11 December 2018)

A string of tracers interacting elastically in a turbulent flow is shown to have a dramatically different behavior when compared to the noninteracting case. In particular, such an elastic chain shows strong preferential sampling of the turbulent flow unlike the usual tracer limit: An elastic chain is trapped in the vortical regions. The degree of preferential sampling and its dependence on the elasticity of the chain is quantified via the Okubo-Weiss parameter. The effect of modifying the deformability of the chain via the number of links that form it is also examined.

DOI: 10.1103/PhysRevLett.121.244501

The development of Lagrangian techniques, in experiments and theory, have lead to major advances in our understanding of the complexity of turbulent flows, especially at small scales [1–3]. What makes this possible is the use of tracer particles which uniformly sample the flow and, hence, access the complete phase space in which the dynamics resides. This feature of tracers depends crucially on the assumption that the particles remain *inertialess* and *pointlike*. When some of these assumptions are relaxed, it may lead to dissipative particle dynamics and preferential sampling of the structures in a flow. This is, for instance, the case for heavy, inertial particles, which show small-scale clustering and concentrate away from vortical regions [4–10]. Various phenomena can influence the properties of inertial clustering in turbulence, such as gravity [11,12], turbophoresis [13,14], or the non-Newtonian nature of the fluid [15]. Preferential sampling in turbulent flows may also emerge as a result of the motility of particles, as in the case of gyrotactic [16], interacting [17], or jumping [18] microswimmers.

We now propose a novel mechanism for preferential sampling in turbulent flows which is induced by extensibility. A simple model of an extensible object which retains enough internal structure is a chain of tracers with an elastic coupling between the nearest neighbors. We show, remarkably, that turning on such elastic interactions amongst tracers leads to very different dynamics: Unlike the case of noninteracting tracers, an elastic chain preferentially samples vortical regions of the flow. We perform a systematic study of this phenomenon and quantify, via the Okubo-Weiss parameter, the level of preferential sampling and its dependence on the elasticity and deformability of the chain.

Harmonic chains have been at the heart of several important problems in the areas of equilibrium and nonequilibrium statistical physics. These have ranged from problems in crystalline to amorphous transitions [19], electrical and thermal transport both in and out of equilibrium [20], as well as understanding the structural properties of disordered and random systems [21]. Given the ubiquity and usefulness of the elastic chain, it is surprising that the effect of a turbulent medium on *long* chains has not been studied as extensively as in other areas of nonequilibrium statistical physics.

There is another reason why this study is important. The last decade or more has seen tremendous advances in our understanding of heavy inertial particles and their dynamics. These were helped primarily by the pioneering results on the issue of preferential concentration, which plays a dominant role in every aspect of turbulent transport. In contrast, similar studies of extended objects such as fibers are recent [22–25], even though they are just as important and commonplace in nature and industry. However, the effect of elasticity, which is intrinsic to extensible objects (just as inertia is to finite-sized particles), in determining their dynamics in a turbulent flow is an open question. In this Letter, we settle this question through a model which is amenable to detailed numerical simulations.

We generalize a well-studied model for polymeric chains, the Rouse model [26–28], which consists of a sequence of N_b identical beads connected through (phantom) elastic links with their nearest left and right neighbors; the two end beads are free. Starting from Newton's equation for a single bead and incorporating the effect of the fluid Stokesian drag, elastic interactions, and thermal noise, the dynamics is most conveniently expressed in terms of the center of mass of the chain $\boldsymbol{X}_c=(\boldsymbol{x}_1+\cdots+\boldsymbol{x}_{N_b})/N_b$ ($\boldsymbol{x}_1,\ldots,\boldsymbol{x}_{N_b}$ denote the positions of the beads) and the separation vector $\boldsymbol{r}_j=\boldsymbol{x}_{j+1}-\boldsymbol{x}_j$ ($j=1,\ldots,N_b-1$) between the jth and $(j+1)$th bead. For arbitrary r_j, the general form of the equations of motion of such a chain in a velocity field $\boldsymbol{u}(\boldsymbol{x},t)$ in the absence of inertia are

$$\dot{\boldsymbol{X}}_c = \frac{1}{N_b}\left(\sum_{i=1}^{N_b} \boldsymbol{u}(\boldsymbol{x}_i, t) + \sqrt{\frac{r_0^2}{2\tau}}\sum_{i=1}^{N_b} \boldsymbol{\xi}_i(t)\right), \tag{1a}$$

$$\dot{\boldsymbol{r}}_j = \boldsymbol{u}(\boldsymbol{x}_{j+1}, t) - \boldsymbol{u}(\boldsymbol{x}_j, t) + \sqrt{\frac{r_0^2}{2\tau}}[\boldsymbol{\xi}_{j+1}(t) - \boldsymbol{\xi}_j(t)] - \frac{1}{4\tau}(2f_j\boldsymbol{r}_j - f_{j+1}\boldsymbol{r}_{j+1} - f_{j-1}\boldsymbol{r}_{j-1}), \tag{1b}$$

where $f_j = (1 - |\boldsymbol{r}_j|^2/r_m^2)^{-1}$ are the standard FENE (finitely extensible nonlinear elastic) interactions [26], which are linear for small separations and diverge quadratically for larger r_j to ensure that interbead separations remain bounded by the maximum length r_m. Thus, at any given instant in time, the length of the chain $R \equiv \sum_j^{N_L} r_j < L_m$, where $L_m = N_L r_m$ is the maximum or contour chain length ($N_L = N_b - 1$ denotes the number of links). The nonlinear elastic links are further characterized by their relaxation time τ, which, in turn, determines the effective relaxation time $\tau_{\text{chain}} = (N_b + 1)N_b\tau/6$ of the chains [29]. The thermal fluctuations on each bead are modeled by independent white noises $\boldsymbol{\xi}_i(t)$ ($i = 1, \ldots, N_b$), whose amplitude r_0 sets the equilibrium length of the chain in the absence of flow. Although the effect of thermal fluctuations on the motion of the center of mass is negligible in a turbulent flow, their effect on the separation vectors is essential: Thermal fluctuations prevent the chain from collapsing into a pointlike particle and, hence, a tracer. Finally, interbead hydrodynamic interactions are ignored.

We note that such a generalized model ensures that when the separations between the beads are small enough for the velocity differences to be approximated as $\boldsymbol{u}(\boldsymbol{x}_{j+1},t) - \boldsymbol{u}(\boldsymbol{x}_j,t) \approx \mathcal{A}\cdot\boldsymbol{r}_j$, where $\mathcal{A}_{ik} = \partial_k u_i$ is the velocity gradient tensor, then Eqs. (1) reduce to the Rouse model with FENE links smaller than the viscous scale at all times. This model is commonly used in simulations of polymer chains in turbulent flows [29–33]. By considering the full velocity difference between adjacent beads, Eqs. (1) describe an elastic chain that may extend into the inertial range of turbulence or even beyond the integral scale [see Refs. [34–37] for an analogous generalization of the dumbbell ($N_b = 2$) model].

What is the effect of a turbulent velocity field $\boldsymbol{u}$ on the motion of such chains? To answer this, we solve, by using a pseudospectral method with a 2/3 dealiasing rule, the two-dimensional Navier-Stokes equation on a square grid with 1024^2 collocation points and 2π periodic boundary conditions. We drive the system to a homogeneous and isotropic, turbulent, statistically steady state through an external, deterministic force $f = -F_0 k_f \cos(k_f x)$ (F_0 is the amplitude and k_f the energy-injection scale in Fourier space, which sets the typical size of the vortices $\ell_f = 2\pi k_f^{-1}$). Forcing at small wave numbers ensures that the vortices are fairly large: This allows us to clearly illustrate the issues of preferential sampling which are central to this work. We use a small Ekmann-friction coefficient μ (in addition to a coefficient of kinematic viscosity ν) to prevent pile up of energy at the large scales due to inverse cascade. Consequently, the turbulent flow is in the direct-cascade regime. The definition of ℓ_f also allows us to characterize the stretching ability of the flow in terms of the dimensionless Weissenberg number $\text{Wi} = \tau_{\text{chain}}/t_f$, where $t_f = \ell_f/\sqrt{2E}$ is the turnover timescale of the large vortices (E is the mean kinetic energy of the flow).

The temporal evolution of the chain [Eqs. (1)] is done by a second-order Runge-Kutta scheme augmented by a rejection algorithm [28] to avoid numerical instabilities due to the divergence of the nonlinear force for $|\boldsymbol{r}_j|$ approaching r_m. A bilinear scheme is used to interpolate, from the Eulerian grid, the fluid velocity at the typically off-grid positions of the beads [38,39]. In order to observe the regime of preferential sampling, we choose parameters for the chain which ensure that its equilibrium length in a quiescent flow is similar to the enstrophy dissipation scale, while $\ell_f < L_m < 2\pi$.

This model of an elastic chain in a turbulent flow is the ideal setting, theoretically and numerically, to investigate the natural interplay between the relative importance of Lagrangian (uniform) mixing and the elasticity of the links. It is this competing effect that leads to a surprising preferential sampling of the flow by the chain, hitherto not observed.

It is important to stress here that we chose two-dimensional turbulent flows to take advantage of their long-lived vortical structures, which help to convincingly illustrate this new phenomenon of preferential sampling. We have checked in several simulations that this phenomenon persists even in three-dimensional turbulence, becoming increasingly prominent as the Reynolds number is raised and intense vortex filaments proliferate. However, as in the case of preferential concentration of inertial particles, the effect is most convincingly brought out in two-dimensional flows.

To illustrate this phenomenon, we begin by randomly seeding 5×10^4 chains into the flow and study their evolution in time for different Wi. (We evolve a large number of chains simultaneously for the purpose of visualizing their sampling behavior and for obtaining good statistics of the chain dynamics; we do not describe the collective motion of an ensemble of chains, which would interact with each other hydrodynamically or by direct contact.) In Fig. 1, we show the center-of-mass positions at an instant of time overlaid on the vorticity field of the turbulent flow for $\text{Wi} = 0.04$ and $\text{Wi} = 0.9$. It is immediately apparent that for the case of small elasticity the chains behave like tracers and distribute evenly [Fig. 1(a)]. However, for larger Wi, there is a preferential sampling of the vortical regions [Fig. 1(b)].

Figure 1(c) demonstrates the coupling between the translational and the extensional dynamics of the chain

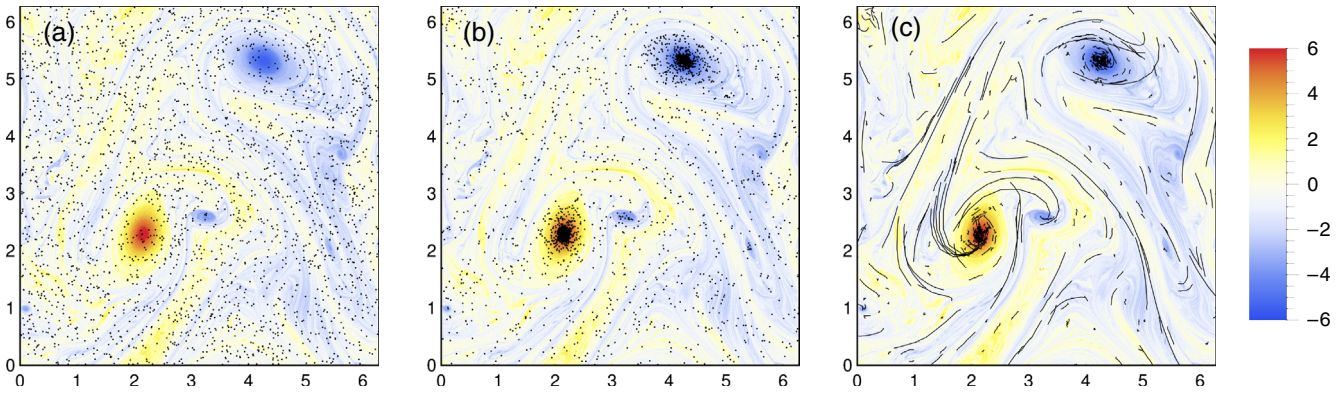

FIG. 1. Representative snapshots showing the positions of a subset of chains ($N_L = 9$ and $L_m = 4$) overlaid on the vorticity field of the carrier turbulent flow (with $\ell_f = 2$ and $t_f = 2.3$). Panels (a) and (b) show the centers of mass of the chains for $\mathrm{Wi} = 0.04$ and $\mathrm{Wi} = 0.9$, respectively. Panel (c) shows the entire chains for $\mathrm{Wi} = 0.9$. Parameter values: $\nu = 10^{-6}$, $\mu = 10^{-2}$, and $F_0 = 0.2$.

by showing a snapshot in which the entire chains, and not just the centers of mass, are overlaid on the vorticity field. This figure emphasises the strong correlation between the positions of elongated chains with regions of low vorticity, where the straining flow stretches out the chains. In contrast, the chains that encounter vortices tend to curl up and contract to a much smaller size. These strikingly different phenomena are best seen in a video of the time evolution of the chains [40]. All of this suggests the following picture: A stretched chain is more likely to leave straining zones and coil up in vortical regions.

The above observations can be quantified via a Lagrangian approach by measuring the statistics of the extension R and the Okubo-Weiss parameter Λ along the trajectories of the centers of mass of the chains. We recall that, for incompressible flows, $\Lambda \equiv \det \mathcal{A}/\langle\omega^2\rangle = (\omega^2 - \sigma^2)/4\langle\omega^2\rangle$ (here rescaled by the mean enstrophy $\langle\omega^2\rangle$), where $\boldsymbol{\omega} = \nabla \times \boldsymbol{u}$ is the vorticity and σ is the strain rate given by $\sigma^2 = 2\mathcal{S}_{ij}\mathcal{S}_{ij}$ where $\mathcal{S} = (\mathcal{A} + \mathcal{A}^T)/2$. The sign of Λ uniquely determines the local flow geometry: For positive Λ, the flow is vortical; for negative Λ, it is extensional [38,41]. Values of Λ near zero correspond to either a quiescent or a shearing flow, which has comparable amounts of vorticity and straining.

In Fig. 2, we show the Lagrangian probability distribution function (PDF) of Λ [Fig. 2(a)] and R [Fig. 2(b)] for different values of Wi. The Λ distribution for tracers ($\mathrm{Wi} = 0$) is also shown for comparison (its positive skewness is a consequence of the strongest velocity gradients occurring in intense vortical zones [42–44]). We find strong quantitative evidence that increasing elasticity leads to a chain preferentially sampling vortical regions of the flow [Fig. 2(a)]. This is accompanied by an increase in the probability of highly stretched configurations [Fig. 2(b)].

The key to understanding the phenomenon of preferential sampling lies in the correlation between the translational and the extensional dynamics of a chain. This is quantified through the joint PDF $P(R, \Lambda)$, which shows that when its center of mass is in vortical regions, a chain is in a contracted state (Fig. 3). The velocity terms in Eq. (1a) can therefore be Taylor expanded about $\boldsymbol{X}_c(t)$, and Eq. (1a) reduces to the equation of motion of a tracer. Thence, the center of mass follows the flow and remains trapped in the

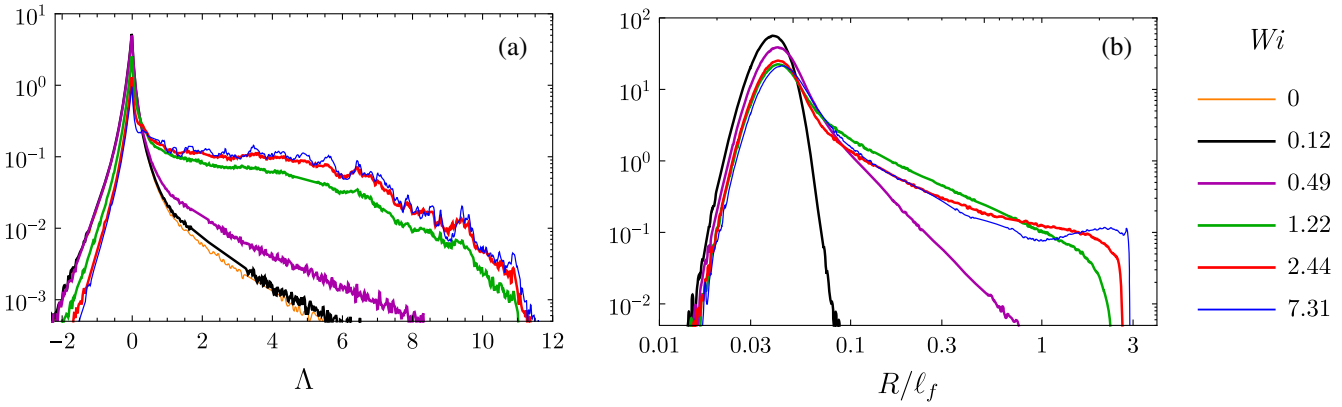

FIG. 2. Lagrangian PDFs of (a) the Okubo-Weiss parameter Λ and (b) the scaled lengths of the chains R/ℓ_f for different values of Wi. Parameter values: $\ell_f = 1.25, t_f = 1.35, L_m = 3.75, N_L = 9$, $\nu = 10^{-6}$, $\mu = 10^{-2}$, and $F_0 = 0.2$.

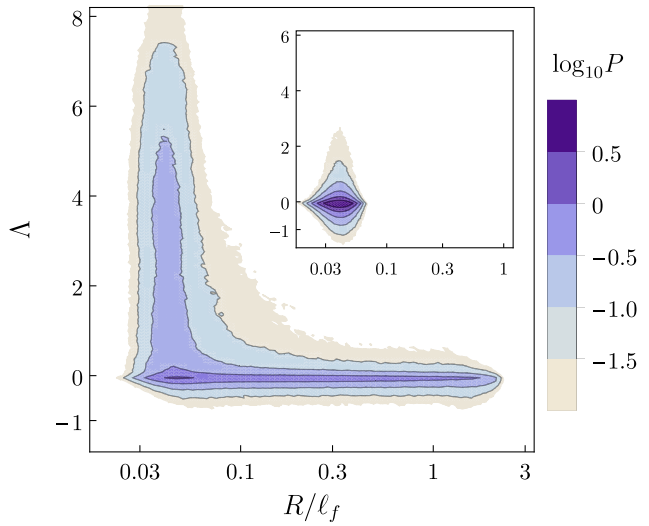

FIG. 3. Joint PDF of Λ sampled by the centers of mass of the chains and R/ℓ_f for Wi = 1.22 and (inset) Wi = 0.12.

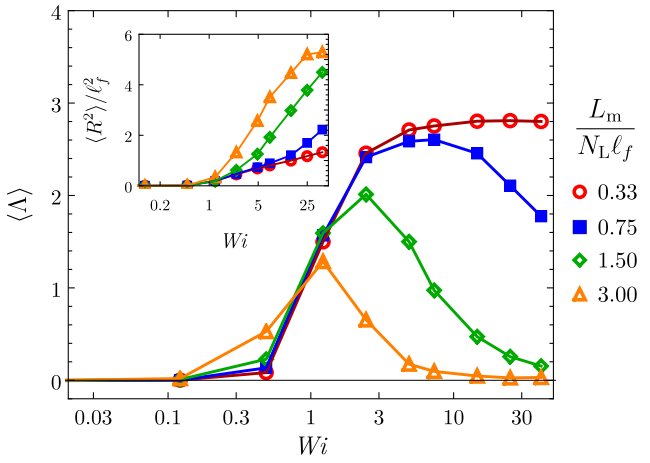

FIG. 4. $\langle\Lambda\rangle$ vs Wi for different values of $\Phi \equiv L_m/(N_L\ell_f)$; we use $N_L = 9$, 4, 2, and 1 (dumbbell), while keeping $L_m = 3.75$ and $\ell_f = 1.25$ fixed. Inset: The variance of R/ℓ_f vs Wi. The flow parameters are the same as those in Fig. 2.

vortex. Contrastingly, away from vortical regions, i.e., in straining or shearing regions, an extensible chain is highly stretched (Fig. 3). As time proceeds, a large-Wi chain stretches to lengths so long that eventually it is unable to follow the rapidly evolving straining zones. On departing from these zones, such a chain is likely to encounter a vortex and begin to coil up (seen clearly in the video [40]). The links of the chain that enter the vortex shrink and follow the rotational flow, eventually leading to the entrapment of the entire chain within the vortex. A stiff chain (small Wi), which remains short in straining zones, samples the negative values of Λ more, leading to annular contours (Fig. 3, inset).

The stretching out of a chain in straining zones may thus be seen as a precursor to its entrapment inside vortices. This explains why strong preferential sampling of vortices occurs only when Wi is so large that there is a significant probability for chains to be stretched beyond ℓ_f (compare the cases of Wi = 0.49 and Wi = 1.22 in Fig. 2). On the other hand, if the maximum length $L_m < \ell_f$, then one would expect this mechanism to fail and the chain to uniformly sample the flow for all Wi. We have confirmed this hypothesis in our simulations but do not show the results for brevity.

The results so far suggest a complete picture for the dynamics of an elastic chain in a turbulent flow: A chain with a sufficient degree of elasticity—defined as the ratio of elastic and fluid timescales—preferentially samples the flow. But is this effect truly independent of the characteristic *length* scales present in the system? The short answer is no, and the ability of a chain to preferentially sample the flow is determined by the relative magnitudes of its typical interbead separation (which for a fixed value of L_m depends only on N_b) and the characteristic fluid length scale ℓ_f.

For large values of Wi, as we have seen, the typical interbead separation approaches L_m/N_L. For the results reported so far, N_b was such that $L_m/N_L \ll \ell_f$. As N_b decreases, however, we will eventually obtain characteristic interbead separations of the order of $L_m/N_L > \ell_f$. In this setting, typically, no two neighboring beads will be able to reside in a vortex simultaneously. Hence, the mechanism for preferential sampling will fail, and the chain will start sampling the flow uniformly once more. This suggests that, apart from the role of elasticity, the dynamics of a chain for large values of Wi ought to depend on a second dimensionless number $\Phi \equiv L_m/(N_L\ell_f)$, such that for $\Phi > 1$ there should be uniform sampling, while for $\Phi < 1$ there should be preferential sampling.

Direct evidence for this is presented in Fig. 4, which shows the mean value of the Okubo-Weiss parameter $\langle\Lambda\rangle$ as a function of Wi for different values of Φ. For smaller Φ, there is an increase in $\langle\Lambda\rangle$ that eventually saturates for Wi $\gtrsim 5$. However, for larger values of Φ, $\langle\Lambda\rangle$ increases initially [45]—indicating preferential sampling of the vortical regions of the flow—before decreasing again to reflect uniform sampling (see video [46]). The chain, however, continues to stretch as the elasticity increases for all values of Φ, and its mean square extension does not show any nonmonotonic behavior (inset of Fig. 4). At large Wi, a chain is indeed typically longer for larger values of Φ owing to the reduced level of preferential sampling of vortices and correspondingly lower probability of being in a contracted state.

Figure 4 lends itself to an intuitively appealing picture of the motion of a chain. For a given turbulent flow (characterized by t_f and ℓ_f), whether or not a chain of a given elasticity and maximum length L_m may coil—and, hence, preferentially sample—depends on the number of links which form the chain. In particular, for a highly extended chain (large Wi), decreasing the number of links limits the ability of the chain to coil up into vortices. This result

highlights the importance of *deformability* of extensible chains. In our study, we have considered a freely jointed chain. However, the bending stiffness of the chain may be modeled by introducing a potential force that is a function of the internal angle between neighboring links and restores them to an antiparallel configuration [26]. Such a stiffness would prevent the chain from coiling up and, therefore, would reduce preferential sampling in a manner analogous to that of increasing Φ in our freely jointed model.

The elastic chain is a simplified model for various physical systems, which include, *inter alia*, fibers, microtubules, and algae in marine environments. Such systems, of course, present additional properties that were not taken into account here, such as the inertia and the stiffness of the system, hydrodynamic and excluded-volume interactions between different portions of it, and the modification of the flow generated by the motion of the system. These effects will certainly change quantitative details of the dynamics, but the mechanism at the origin of preferential sampling identified here is of general validity. It indeed relies on a few basic ingredients: The system must be extensible, its equilibrium size should be smaller than ℓ_f, and its contour length greater than ℓ_f.

Finally, we cannot avoid mentioning that the preferential concentration of inertial particles through dissipative dynamics is completely different from the mechanism that we report here. Hence, it is tempting to investigate the interplay between the competing effects of inertia and elasticity in future studies of inertial extensible objects in turbulent flows.

We thank Abhishek Dhar, Anupam Kundu, and Rahul Pandit for useful suggestions and discussions. We acknowledge the support of the Indo-French Centre for Applied Mathematics. S. S. R. acknowledges Department of Science and Technology (DST) (India) Project No. ECR/2015/000361 for financial support. J. R. P. acknowledges travel support from the International Centre for Theoretical Sciences (ICTS) Infosys Collaboration grant. The simulations were performed on the ICTS clusters *Mowgli* and *Mario*, as well as the work stations from the Project No. ECR/2015/000361: *Goopy* and *Bagha*.

*jrpicardo@icts.res.in
†dario.vincenzi@unice.fr
‡nairitap2009@gmail.com
§samriddhisankarray@gmail.com

[1] P. K. Yeung, Annu. Rev. Fluid Mech. **34**, 115 (2002).
[2] F. Toschi and E. Bodenschatz, Annu. Rev. Fluid Mech. **41**, 375 (2009).
[3] J. P. L. C. Salazar and L. R. Collins, Annu. Rev. Fluid Mech. **41**, 405 (2009).
[4] E. K. Longmire and J. K. Eaton, J. Fluid Mech. **236**, 217 (1992).
[5] J. Bec, Phys. Fluids **15**, L81 (2003); J. Fluid Mech. **528**, 255 (2005).
[6] J. Bec, A. Celani, M. Cencini, and S. Musacchio, Phys. Fluids **17**, 073301 (2005).
[7] J. Chun, D. L. Koch, S. L. Rani, A. Ahluwalia, and L. R. Collins, J. Fluid Mech. **536**, 219 (2005).
[8] J. Bec, L. Biferale, M. Cencini, A. Lanotte, S. Musacchio, and F. Toschi, Phys. Rev. Lett. **98**, 084502 (2007).
[9] R. Monchaux, M. Bourgoin, and A. Cartellier, Int. J. Multiphase Flow **40**, 1 (2012).
[10] K. Gustavsson and B. Mehlig, Adv. Phys. **65**, 1 (2016).
[11] J. Bec, H. Homann, and S. S. Ray, Phys. Rev. Lett. **112**, 184501 (2014).
[12] G. H. Good, P. J. Ireland, G. P. Bewley, E. Bodenschatz, L. R. Collins, and Z. Warhaft, J. Fluid Mech. **759**, R3 (2014).
[13] S. Belan, I. Fouxon, and G. Falkovich, Phys. Rev. Lett. **112**, 234502 (2014).
[14] F. De Lillo, M. Cencini, S. Musacchio, and G. Boffetta, Phys. Fluids **28**, 035104 (2016).
[15] F. De Lillo, G. Boffetta, and S. Musacchio, Phys. Rev. E **85**, 036308 (2012).
[16] W. M. Durham, E. Climent, M. Barry, F. De Lillo, G. Boffetta, M. Cencini, and R. Stocker, Nat. Commun. **4**, 2148 (2013).
[17] A. Choudhary, D. Venkataraman, and S. S. Ray, Europhys. Lett. **112**, 24005 (2015).
[18] H. Ardeshiri, I. Benkeddad, F. G. Schmitt, S. Souissi, F. Toschi, and E. Calzavarini, Phys. Rev. E **93**, 043117 (2016).
[19] Z. H. Stachurski, Materials **4**, 1564 (2011); B. Illing, S. Fritschi, H. Kaiser, C. L. Klix, G. Maret, and P. Keim, Proc. Natl. Acad. Sci. U.S.A. **114**, 1856 (2017).
[20] A. Dhar, Phys. Rev. Lett. **86**, 5882 (2001); S. Lepri, R. Livi, and A. Politi, Phys. Rep. **377**, 1 (2003); A. Dhar, Adv. Phys. **57**, 457 (2008); A. Kundu, S. Sabhapandit, and A. Dhar, J. Stat. Mech. (2011) P03007.
[21] A. M. Mayes, Macromolecules **27**, 3114 (1994); K. Binder, J. Baschnagel, and W. Paul, Prog. Polym. Sci. **28**, 115 (2003); P. Chaudhuri, S. Karmakar, C. Dasgupta, H. R. Krishnamurthy, and A. K. Sood, Phys. Rev. Lett. **95**, 248301 (2005); T. Sridhar, D. A. Nguyen, R. Prabhakar, and J. R. Prakash, Phys. Rev. Lett. **98**, 167801 (2007).
[22] C. Brouzet, G. Verhille, and P. Le Gal, Phys. Rev. Lett. **112**, 074501 (2014).
[23] G. Verhille and A. Bartoli, Exp. Fluids **57**, 117 (2016).
[24] M. E. Rosti, A. A. Banaei, L. Brandt, and A. Mazzino, Phys. Rev. Lett. **121**, 044501 (2018).
[25] S. Allende, C. Henry, and J. Bec, Phys. Rev. Lett. **121**, 154501 (2018).
[26] R. B. Bird, C. F. Curtiss, R. C. Armstrong, and O. Hassager, *Dynamics of Polymeric Liquids* (John Wiley and Sons, New York, 1977), Vol. 2.
[27] M. Doi and S. F. Edwards, *The Theory of Polymer Dynamics* (Oxford University Press, Oxford, 1986).
[28] H. C. Öttinger, *Stochastic Processes in Polymeric Fluids* (Springer, Berlin, 1996).
[29] J. Jin and L. R. Collins, New J. Phys. **9**, 360 (2007).
[30] H. Massah, K. Kontomaris, W. R. Schowalter, and T. J. Hanratty, Phys. Fluids A **5**, 881 (1993).

[31] Q. Zhou and R. Akhavan, J. Non-Newtonian Fluid Mech. **109**, 115 (2003).
[32] V. K. Gupta, R. Sureshkumar, and B. Khomami, Phys. Fluids **16**, 1546 (2004).
[33] T. Watanabe and T. Gotoh, Phys. Rev. E **81**, 066301 (2010).
[34] M. De Lucia, A. Mazzino, and A. Vulpiani, Europhys. Lett. **60**, 181 (2002).
[35] M. F. Piva and S. Gabanelli, J. Phys. A **36**, 4291 (2003).
[36] J. Davoudi and J. Schumacher, Phys. Fluids **18**, 025103 (2006).
[37] A. Ahmad and D. Vincenzi, Phys. Rev. E **93**, 052605 (2016).
[38] P. Perlekar, S. S. Ray, D. Mitra, and R. Pandit, Phys. Rev. Lett. **106**, 054501 (2011).
[39] M. James and S. S. Ray, Sci. Rep. **7**, 12231 (2017).
[40] https://youtu.be/etLuK6ovAqk.
[41] A. Okubo, Deep-Sea Res. Oceanogr. Abstr. **17**, 445 (1970); J. Weiss, Physica (Amsterdam) **48D**, 273 (1991).
[42] P. Perlekar and R. Pandit, New J. Phys. **11**, 073003 (2009).
[43] A. Gupta, P. Perlekar, and R. Pandit, Phys. Rev. E **91**, 033013 (2015).
[44] D. Mitra and P. Perlekar, Phys. Rev. Fluids **3**, 044303 (2018).
[45] See also Refs. [34,35] for dumbbells in cellular flows.
[46] Online video showing uniform sampling of highly stretched dumbbells, https://youtu.be/YdFXMFFU1qU.